



© 2023. The Author(s). This is an open-access article distributed under the terms of the Creative Commons Attribution-ShareAlike 4.0 International Public License (CC BY SA 4.0, <https://creativecommons.org/licenses/by-sa/4.0/legalcode>), which permits use, distribution, and reproduction in any medium, provided that the article is properly cited.

Study of Zn(II) ion removal from galvanic sludge by geopolymers

Elżbieta Sitarz-Palczak

Rzeszow University of Technology, Poland

* Corresponding author's e-mail: epalczak@prz.edu.pl

Keywords: waste, fly ash, geopolymer

Abstract: The galvanic sludges contain a number of toxic heavy metals, potentially mobilized as chemically active ions under environmental conditions as. This study explores the application of fly ash-based geopolymers for the removal of Zn ions from galvanizing sludge. In this study, geopolymers, synthesized via the geopolymerization method, were used to remove Zn from post-galvanized sewage sludge. Two types of geopolymers were used, derived from ash from coal combustion and biomass combustion. Structural, morphological, and surface properties were characterized using FTIR and SEM, respectively. In addition, BET and Langmuir isotherms, along with analyses such as t-Plot and BJH method for porous solids were conducted. The results indicate that the geopolymer derived from coal combustion ash is a more effective sorbent for Zn(II) ions, exhibiting a removal efficiency of 99.9%, compared to 40.7% for the geopolymer derived from biomass combustion ash. The FTIR spectra analysis reveals the presence of bonds between the -OH and/or Si-OH groups on the geopolymers' surface and the Zn(II) ions. The environmentally and economically advantageous process maximizes the recovery of a valuable component at minimal cost, yielding relatively clean monometallic waste suitable for reuse.

Introduction

Waste from the electroplating industry deserves special attention due to its high environmental impact. Electroplating is the production of permanently adherent thin metallic coatings by depositing one metal on another (e.g., chromium plating, zinc plating, cadmium plating). During the processes carried out in electroplating plants, large amounts of galvanic sewage containing cations of various metals are generated, which classifies it as hazardous to the environment (Świerk et al. 2007). Galvanic sewage sludges have a different chemical composition, depending on the production process and the type of reactants used in the neutralization of this type of waste (Letcher and Vallero 2019). They fall into the category of hazardous waste, which can be treated using biological methods (Luo et al. 2017, Ayilara et al. 2020) thermal techniques (Irisawa et al. 2021, Butenegro et al. 2021), and chemical processes (Jarnerud et al. 2021, Riaz et al. 2020). Additionally, galvanic sewage sludge can be landfilled after conversion to inert material (Rybak et al. 2021, Nanda and Berruti 2021).

Post-neutralization sludge is amorphous, with its composition being predominantly composed of hydroxides and carbonates (Krstič et al. 2018). A small portion of the sludge, characterized by higher concentrations of sulphate (VI) ions, also forms crystalline substances such as CaSO_4 (Stepanov et al. 2016). These sludges belong to hazardous wastes but are

also a valuable source of various metals, including copper, zinc, nickel, cadmium, gold, and silver. Classified as toxic heavy metals, they can be mobile under environmental conditions as chemically active ions. The presence of heavy metals requires the recycling of these wastes and the reuse of the heavy metals they contain. Metals present in the galvanic sludge that cannot be recycled or reused must be immobilized prior to storage. Metal immobilization techniques are environmentally friendly solutions but do not allow the recovery of valuable components. There is a large body of work dedicated to studying the treatment and disposal of industrial waste residues, particularly galvanic sludge (Makisha and Yunchina 2017, Rossini and Bernardes 2006, Sanito et al. 2022). The main treatment and disposal methods include pyrometallurgical (Yang et al. 2022, Kwon and Sohn 2020, Barakat 2003), hydrometallurgical, and bio-hydrometallurgical processes (Dvořák and Jandova 2005, Jha et al. 2001, Rudnik 2019). The stabilization of toxic metals in post-galvanic wastes takes place using various techniques, one of which is solidification, i.e., immobilization in a solid matrix by means of lime hydrate or cement (bituminating in solidified melt (Bednarik et al. 2005), cementation (Luz et al. 2009, Stepanov et al. 2016,), vitrification (Irisawa et al. 2021, Krstič et al. 2018, Sanito et al. 2022)). Combined methods also deserve attention because they allow the problem of galvanic sludge to be solved and the search for an optimal process for recovering elements from this sludge with the highest possible purity (Krishnan et al. 2021).

The issue of treating galvanic sludge is highly relevant, with a growing emphasis on finding the most effective method for recycling and utilizing each valuable metal. The research carried out in this thesis focused on the use of geopolymers derived from coal combustion ash and biomass combustion. Geopolymers are amorphous structures that typically manifest as hard, mechanically resistant solids, resembling natural stone or concrete in appearance. While much scientific attention has been given to studying their mechanical properties, these materials show other interesting characteristics, suggesting their potential application in innovative areas such as wastewater treatment and toxic waste immobilization (Imtiaz et al. 2020; Khan et al. 2021).

Considering the results of previous studies on the sorption properties of geopolymers (Sitarz-Palczak et al. 2019), this research investigated the potential use of geopolymers derived from coal combustion ash and biomass combustion to extract zinc(II) ions from galvanic sludge through leaching and subsequent adsorption on the surface of geopolymers. Zinc exists in readily soluble forms, posing an additional source of contamination for both soils and waters in galvanizing waste. Approximately 80% of the world's zinc production is used for steel galvanization prior to the corrosion process (Sinha et al. 2020). Given the high zinc content, galvanic wastes can be considered valuable secondary raw materials, justifying the exploration of new methods for recovering Zn from these waste materials. The recovery of zinc from electroplating waste not only yields economic benefits but also contributes to the neutralization of the hazardous waste, specifically galvanic sludge, aligning with desirable environmental goals.

Materials and methods

Materials

The materials used in this study were galvanic sludge (GS), geopolymers based on coal combustion ash (PW/GEO), or biomass (PB/GEO).

The galvanic sludge was obtained from the wastewater treatment plant at the Koelner Screw Factory (Łańcut, Poland). The sludge is produced by two processes: in the pickling plant and in the electroplating plant. In the pickling plant, wires used in the production of screws are washed with 15% sulphuric acid(VI) to clean and de-rust the rods. After the pickling process, the rods are rinsed with a large volume of water. The acidified water is sent to a wastewater treatment plant and then neutralized with a prepared $\text{Ca}(\text{OH})_2$ solution. In the electroplating process, chromium and zinc are used for coating. The products are washed with a large amount of water, resulting in some of the chromium and zinc salts entering the water. The water then flows to a wastewater treatment plant, where the salts are precipitated with a $\text{Ca}(\text{OH})_2$ solution. In the treatment plant, the solutions are mixed, and solid and semi-liquid impurities are separated, which are then transported to a warehouse and taken to a storage area. For a detailed characterization of the physico-chemical properties, morphology, and chemical composition of the post-plating sludge, refer to the paper (Galas et al 2016). The sludge was dried at room temperature for a period of 30 days to an air-dry state and then crushed in a ceramic and agate mortar ($\varphi \leq 100 \mu\text{m}$).

Coal and biomass combustion by-products, namely coal fly ash (PW) and biomass combustion fly ash (PB), served

as the starting raw materials for geopolymer synthesis. These materials are a source of reactive silica and alumina, providing a binder for the geopolymer matrix. They were used in the form of a solid mixture composed of equal parts by weight of quartz sand and the respective starting raw material. An alkali activator, consisting of a mixture of sodium silicate (with a $\text{SiO}_2 + \text{Na}_2\text{O}$ content of not less than 39% by weight and $\text{SiO}_2/\text{Na}_2\text{O}$ molar modulus of 2.4 - 2.6) and solid sodium hydroxide (with a purity of 97% by weight) was used. To create the geopolymer paste, the mixture of solid components was mixed with an alkaline activator at a 50:50 ratio of aqueous phase [cm³] to solid phase [g]. Once a homogeneous mixture was obtained, the geopolymer mortars were transferred into 14 mm × 10 mm cylindrical molds. The samples were removed from the molds after 24 h and then cured at ambient temperature (~20 °C) and humidity (~68%) for 28 days. A description of the synthesis of geopolymers based on coal combustion and biomass combustion ash along with the results from surface morphology and chemical composition analyses, as well as sorption and catalytic properties are presented in detail in paper (Sitarz-Palczak et al. 2019). Prior to the sorption experiment, the geopolymer samples were brought to constant mass under laboratory conditions.

Methods

The structure, morphology, and surface properties of the materials used were characterized using Scanning Electron Microscopy (SEM) and Fourier Transform Infrared Spectroscopy (FTIR), respectively. Elemental composition analysis was performed through Energy Dispersive X-ray Spectroscopy (EDS). For microstructure and chemical composition determination of the galvanic sludge and geopolymer samples, an SEM (Hitachi S-3400N) equipped with an energy-dispersive X-ray spectroscopy detector (EDS) was employed. Samples were prepared by placing them on a carbon belt with gold sputtering.

The infrared absorption spectra were recorded at the basic level in the range of 4000 - 400 cm^{-1} with a resolution of 2 cm^{-1} using a Bruker (Germany) FTIR ALPHA spectrometer. Powder preparations for the analysis were created by mixing approx. 0.5 mg of the analyzed sample with 200 mg of spectrally pure KBr. The resulting mixture was formed into a pill by subjecting it to vacuum conditions at a pressure of 10 MPa.

Total zinc content

To determine the total zinc content of the test materials, a one-step mineralization was performed using a mixture of concentrated acids (HClO_4 , HF and H_2O) in a volume ratio of 2:2:1. The process was carried out using Teflon crucibles on an electric plate at 98°C under atmospheric pressure until the acid mixture was completely evaporated. After mineralization, the solutions were filtered through an analytical sieve for quantitative analysis and then acidified with 1 cm^3 HNO_3 at a concentration of 2 mol/dm^3 . Zinc determinations in aqueous solutions were carried out using Flame Atomic Absorption Spectrometry (FAAS) with a Perkin-Elmer 3100 Model flame atomic absorption spectrometer (Shelton Instruments, CT USA). The determination of total Zn was conducted in two parallel samples, and the reported result is the average of the two determinations.

In addition, the BET and Langmuir isotherms, as well as the analysis of these isotherms for porous solids (t-Plot method and BJH method) were conducted. Nitrogen sorption isotherms of geopolymers were measured with ASAP 2420 (Micromeritics Instrument Corporation, Norcross, USA) apparatus, at a temperature of 196°C. Prior to the sorption measurements, all samples were degassed at 120°C for at least 24 hours at a pressure of 10^{-3} Pa.

Experiment on the adsorption of zinc from galvanic sludge by geopolymers

Building on preliminary studies conducted on the electroplating sludge, which involved leaching with deionized water at different pH values (Galas et al 2016), and considering the insights gained from the examination of the resulting geopolymers in terms of the heavy metal adsorption mechanism (Sitarz-Palczak et al 2019), the experiment was designed to replicate near-real conditions, specifically environmental conditions. For the experiment, 40.00 g of galvanic sewage sludge (GS) was weighed and 30 cm³ each of deionized water was added to achieve a moisture content close to the actual moisture content. The same procedure was followed for coal combustion ash-based geopolymer (PW/GEO) and biomass combustion ash-based geopolymer (PB/GEO) each in separate sludge samples. Geopolymer shapes, each measuring 14x10 mm and weighing approximately 2.00 g, were used. To ensure the accuracy of the analyses, 3 control samples were prepared to eliminate the possibility of an accidental phenomena affecting the results. The experiment was conducted for a period of 30 days, during which the system was supplemented with 17 cm³ of deionized water every 7 days, which corresponds to the average amount of rainfall per year in Poland. After one month, the geopolymers were removed from the galvanic sludge, dried at room temperature, and then ground and grinded in a porcelain and agate mortar. The prepared samples underwent FTIR and SEM/EDS spectroscopic analysis. Furthermore, all samples (GS, PW/GEO, and PB/GEO) were mineralized using a mixture of concentrated acids (HClO₄, HF and H₂O). The Zn content of the resulting solutions was determined by atomic absorption spectroscopy (FAAS). Total Zn content determinations were conducted in two parallel samples, and the reported result is the average of the two determinations.

Results and discussion

Scanning Electron Microscopy/Energy Dispersive X-ray Spectroscopy (SEM/EDS)

SEM analysis of the microstructure of the geopolymer obtained from coal combustion ash after adsorption of Zn(II) ions (Figure 1), shows the complex morphology characteristic of this material. A trait typical of this group of materials (Pu et al. 2016). Notably, a high surface heterogeneity can be observed, which is attributed to the diverse grain structure of coal combustion ash and the presence of amorphous silicates, resulting in a porous surface. In addition, the micrographs also reveal the presence of particle conglomerates, minerals, and mineral aggregates. The particle size range is very wide, from below 1 μm to above 200 μm. Figure 2 presents the results of the chemical analysis by EDS. Oxygen, aluminum,

silicon, potassium, iron, and zinc were found in all areas, with the additional presence of calcium in areas 3 - 4 and sodium in area 1. Silicon dominates in all areas (15.1 - 31.0 wt.%). Zinc content varies across areas from 3.2 - 52.5%. The lowest content of Zn(II) adsorbed on the surface of the geopolymer obtained from coal combustion ash was found in spherical forms, which have the highest content of silicate ions and aluminum ions. In contrast, the highest zinc ion content was found in amorphous porous forms, characterized by the lowest silicate and aluminum ion content.

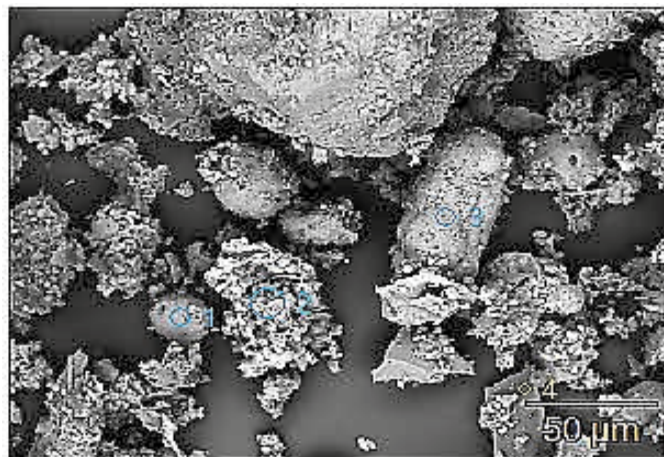


Figure 1. SEM image of the PW/GEO geopolymer after adsorption of Zn(II) ions

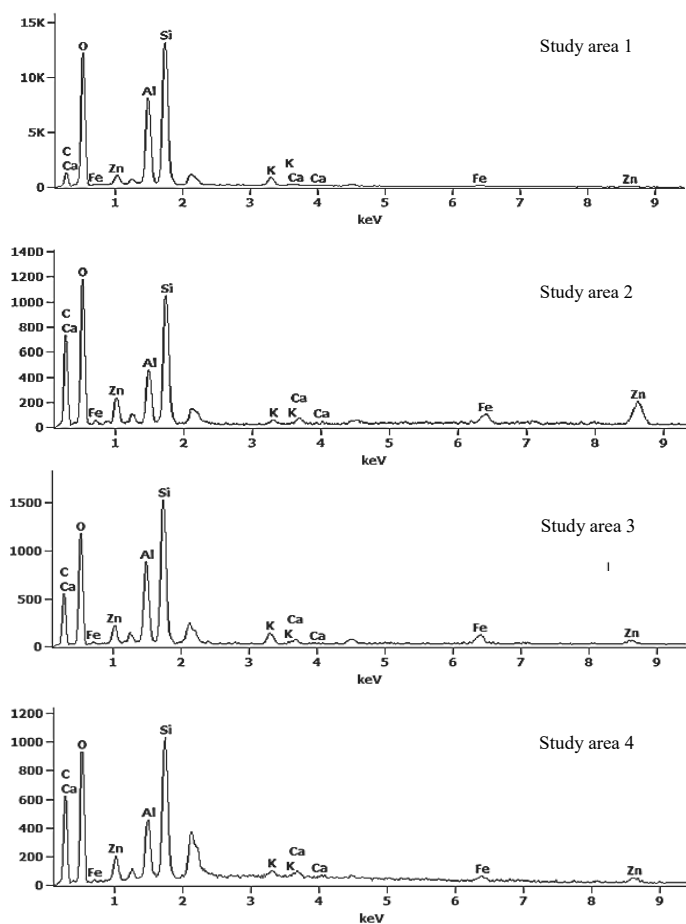


Figure 2. EDS analysis (study areas 1-4) for PW/GEO geopolymer after adsorption of Zn(II) ions

Figure 3 shows an SEM image of the geopolymer microstructure obtained from biomass combustion ash after adsorption of Zn(II) ions. The surface of the visible aggregates is heterogeneous, which is due to the diverse grain structure of the ash. In addition, microcracks are visible on the aggregates, which were formed after evaporation of water from the geopolymer matrix (Alehyen et al. 2017). Bright areas rich in calcium and zinc phases, and dark areas rich in aluminosilicate phases are visible on the surface of most aggregates. The particle size range is very wide, from 5 μm to above 100 μm . The results of the EDS chemical analysis are shown in Figure 4. Aluminum, silicon, calcium, and zinc were found in all areas. The dominant contribution in all areas is shown by silicon (approximately 22.9 wt.%). The zinc content accounts for 24.9 wt.%.

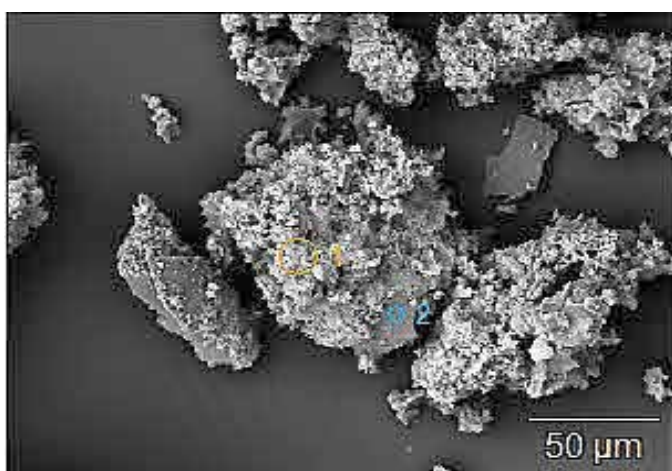


Figure 3. SEM image of the PB/GEO geopolymer after adsorption of Zn(II) ions.

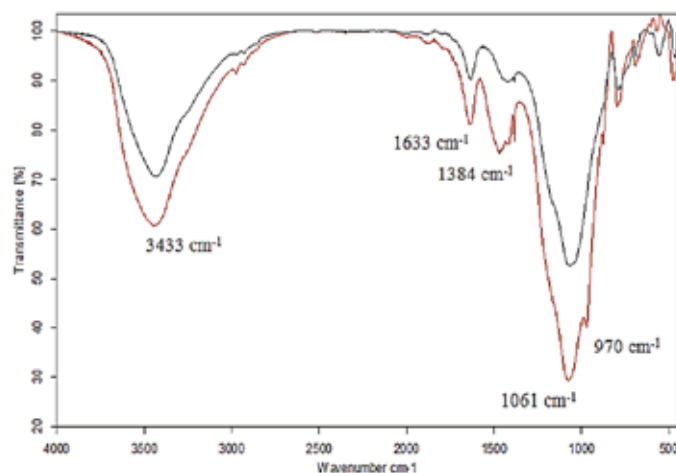


Figure 5. FTIR spectra of geopolymers before sorption of Zn(II) ions (PW/GEO – color black and PB/GEO – color red).

The spectra of samples of the applied geopolymers (PW/GEO and PB/GEO) before and after sorption of Zn(II) ions were compared. These comparisons are shown sequentially in Figures 5 and Figures 6 and 7. The key adsorption bands observed on the spectrograms after the sorption of Zn(II) ions by PW/GEO, concerning a sample of this geopolymer before the sorption experiment, are summarized in Table 1. An analogous summary is given in Table 2 for a sample of biomass combustion geopolymer (PB/GEO) before and after the sorption experiment. The FTIR spectra of PW/GEO and PB/GEO before the sorption experiment contain identical adsorption bands. In the spectra, two prominent high-intensity bands are observed, namely a distinct broad band in the wavelength range of 4000 – 2850 cm^{-1} , which arises from the stretching vibrations of aliphatic -CH groups, -OH groups of alcohols, phenols. Additionally, it may originate from hydrogen bonds and the stretching vibrations of H-O-H water molecules adsorbed on the sample surface. An increase in the intensity of this band indicates an increase in the water content of the geopolymer samples prior to the sorption experiment. The band around 970 cm^{-1} signifies characteristic aluminum-silicon skeleton, specifically the asymmetric Si-O stretching vibrations. The presence of an adsorption band at a wavelength of about 1600 cm^{-1} can be attributed to the bending vibrations of H-O-H, indicating the presence of surface-bound water adsorbed on the sorbent surface. In for the case of PB/GEO after the sorption experiment, the disappearance of the band at a around 1640 cm^{-1} , associated with the stretching vibrations of the C=O bond, suggests a reduction in the sorption properties of the material under study. The decreased intensity of the adsorption band around 1420 cm^{-1} may be linked to the blocking of C-O or amide N-H groups due to the adsorption of metal ions on the surface of geopolymers (Brylewska et al. 2018, Zehua et al. 2020).

Following the adsorption of Zn(II) ions by PW/GEO and PB/GEO geopolymers, the FTIR spectrum exhibits changes in four bands for PW/GEO (Table 1) and eight bands for PB/

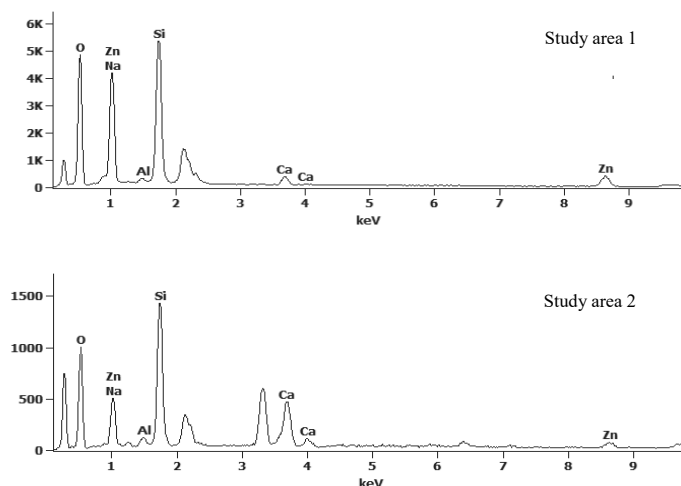


Figure 4. EDS analysis (study areas 1-2) for PB/GEO geopolymer after adsorption of Zn(II) ions.

Fourier Transform Infrared Spectroscopy (FTIR)

The sorption capacity of geopolymers is attributed to the presence of distinctive functional groups that have the capacity to bind a selected group of ions from aqueous solutions. In an aqueous environment, functional groups, such as hydroxyl or

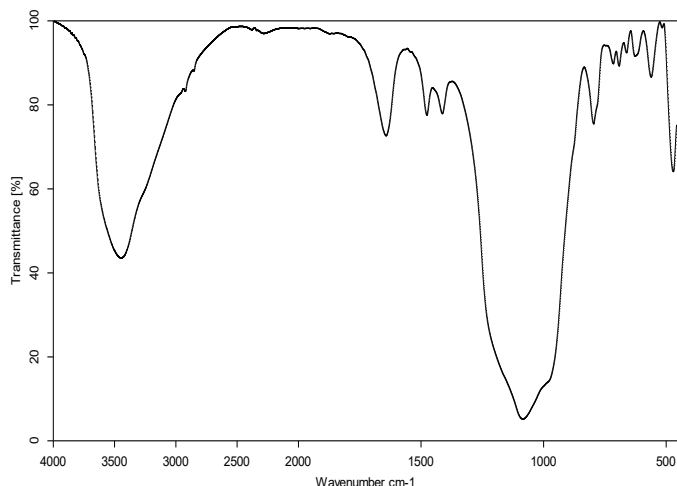


Figure 6. FTIR spectra of geopolymer PW/GEO after sorption of Zn(II) ions.



Figure 7. FTIR spectra of geopolymer PB/GEO after sorption of Zn(II) ions.

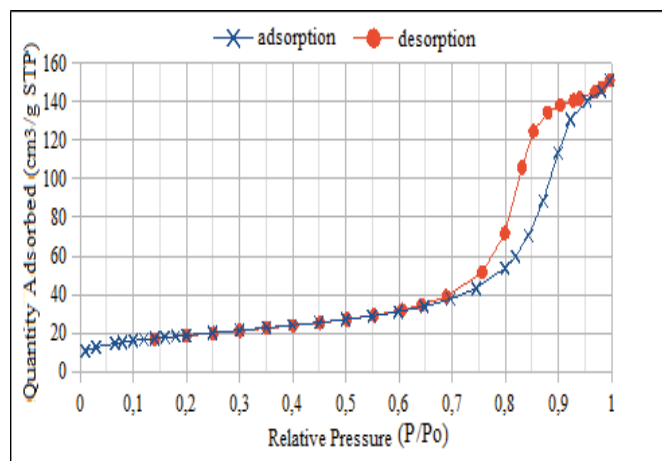


Figure 8. Nitrogen adsorption and desorption isotherms for PW/GEO after adsorption of Zn(II) ions determined by the BET method.

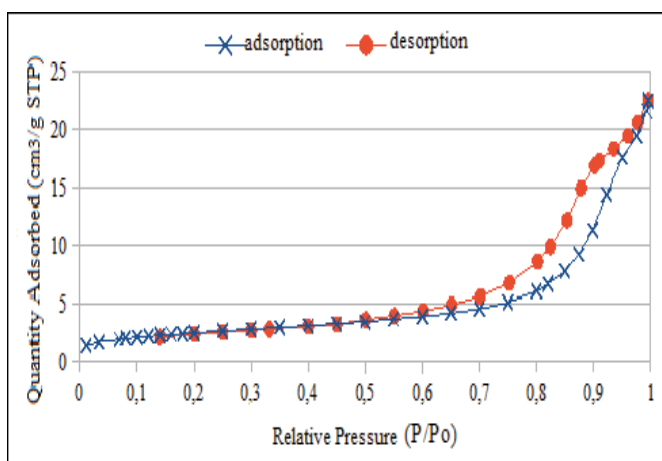


Figure 9. Nitrogen adsorption and desorption isotherms for PB/GEO after adsorption of Zn(II) ions determined by the BET method.

GEO (Table 2). The observable differences primarily involve alterations in intensity and band shifts, particularly in relation to the stretching vibrations of the O-H, C-O and N-H groups. These changes strongly suggest the direct involvement of these functional groups in the adsorption of Zn(II) ions.

Investigations of the porous structure of geopolymers after adsorption of Zn(II) ions

Figures 8 and 9 illustrate the low-temperature nitrogen adsorption isotherms for geopolymers obtained from coal combustion ash (PW/GEO) and biomass combustion ash (PB/GEO) after adsorption of Zn(II) ions. Their shape corresponds to the type IV isotherm according to the IUPAC classification, characteristic of mesoporous adsorbents. In addition, Figure 9 shows the adsorption hysteresis (type H3), indicative of distinct course for adsorption (during pressurization) and desorption (during depressurization) isotherms. This hysteresis type is characteristic of pores shaped like double-sided open slits or cylinders (Donohue and Aranovich 1998).

These geopolymers, in addition to the developed microporosity, have a well-developed mesoporosity. According

to the literature data, the presence of water in the reaction mixture results in the macroporosity of geopolymers. The macropores can transform into mesopores during the polycondensation of the hydrated geopolymer gel (Gao et al. 2014).

Figures 10 and 11 depict the BET adsorption isotherm across a range of relative pressures from 0.05 to 0.25 mmHg. These isotherms were used to determine the specific surface area for geopolymers obtained from coal combustion ash (PW/GEO) and biomass combustion ash (PB/GEO) after Zn adsorption. The observed small specific surface area and pore volume suggest a dense geopolymer matrix. This means that the geopolymers tested have low permeability and consequently high durability (Alehyen et al. 2017).

In Table 3, the results of porosimetry tests, including specific surface area, volume and pore size for the tested geopolymers, are presented. Comparing the geopolymers after Zn(II) ion adsorption (Zn/PW/GEO and Zn/PB/GEO) in terms of the BET surface area, values of 87.06 and 68.20 m²/g were obtained for Zn/PW/GEO and Zn/PB/GEO, respectively. The total micropore area, determined by the t-method for the applied geopolymers after adsorption of Zn(II) ions, is 75.97 m²/g for Zn/PW/GEO

Table 1. Comparison of the main adsorption bands occurring after sorption of Zn(II) ions by PW/GEO with regard to the sample before the sorption experiment.

Band position [cm ⁻¹]	Types of vibration	
	before sorption	after sorption
4000 - 2500	stretching vibrations of the –OH, groups and valence vibrations of the O-H, N-H, C-H bonds	
	wide, very intensity	narrow, less intensity
2249	symmetric stretching vibrations related to the –CH ₂ and –CH groups	band disappears
1700 - 1630	related to the C=O stretching vibrations and N-H bending vibrations	
~ 1600	associated with bending vibrations of the H-O-H groups	
	sharp, low intensity	
1550 - 850	asymmetric and symmetric vibrations of the Si(Al)-O bonds	
1500 - 1400	stretching vibrations of the C-O groups	
~ 1450	scissor vibrations of the –CH ₂ bonds	
	narrow, sharp, low intensity	very low intensity
~ 970	associated with asymmetric stretching vibrations of the (Al)Si-O-Si bonds	band disappears
1200 - 450	internal vibrations of the Si-O(Si) and Si-O(Al) in quadrangular oxygen bridges	

Table 2. Comparison of the main adsorption bands occurring after sorption of Zn(II) ions by PB/GEO with regard to the sample before the sorption experiment.

Band position [cm ⁻¹]	Types of vibration	
	before sorption	after sorption
4000 - 2500	stretching vibrations of the –OH, groups and valence vibrations of the O-H, N-H, C-H bonds	
	wide, very intensity	narrow, less intensity
2249	symmetric stretching vibrations related to the –CH ₂ and –CH groups	band disappears
1700 - 1630	related to the C=O stretching vibrations and N-H bending vibrations	band disappears
~ 1600	associated with bending vibrations of the H-O-H groups	band disappears
1550 - 850	asymmetric and symmetric vibrations of the Si(Al)-O bonds	
	sharp, medium intensity	mild, medium intensity
1500 - 1400	stretching vibrations of the C-O groups	
	narrow, medium intensity	mild, lower intensity
~ 1450	scissor vibrations of the –CH ₂ bonds	
~ 970	associated with asymmetric stretching vibrations of the (Al)Si-O-Si bonds	band disappears
1200 - 450	internal vibrations of the Si-O(Si) and Si-O(Al) in quadrangular oxygen bridges	band disappears

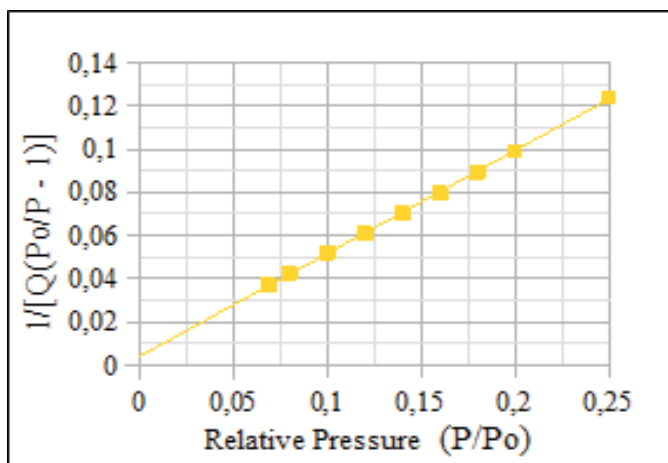


Figure 10. Linear form of the BET adsorption isotherm for PW/GEO after adsorption of Zn(II) ions.

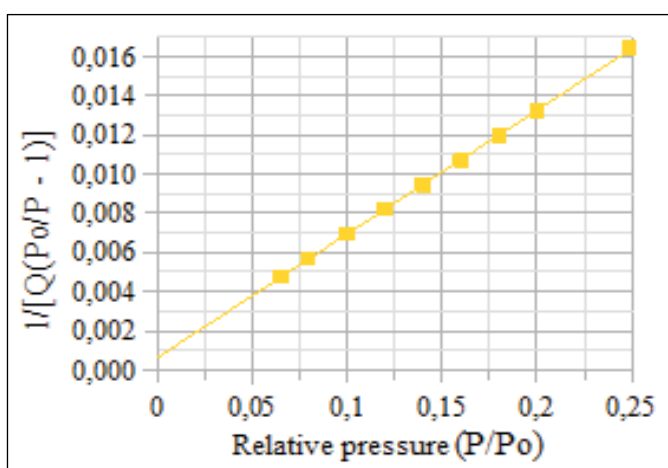


Figure 11. Linear form of the BET adsorption isotherm for PB/GEO after adsorption of Zn(II) ions.

and 65.72 m²/g for Zn/PB/GEO. These values represent 87.26% of the specific surface area of the PW/GEO geopolymer and 96.36% of the specific surface area of the PB/GEO geopolymer, respectively. The lower values obtained for BET specific surface area, microporosity surface area and microporosity volume suggest that mesoporosity is the predominant type of porosity in Zn/PB/GEO samples, while microporosity is the predominant type of porosity in Zn/PW/GEO samples.

These properties have been confirmed in the works (Akono et al. 2019, Luukkonen et al 2016). Given the similar values of the determined structural parameters of both geopolymers, it can be assumed that the mechanism of the metal adsorption process is likely to be similar.

Adsorption of zinc from galvanic sludge

The adsorption of Zn(II) ions varied with respect to the utilized geopolymers. This is evident from the removal efficiencies zinc ions, which were 99.9% for PW/GEO and 40.7% for PB/GEO, respectively (Table 4). The obtained results indicate the complete removal of Zn(II) ions, which shows that the efficiency of the adsorption process of Zn(II) ions by the geopolymer from coal combustion ash is very high.

The results obtained were compared with data from the literature. In a study (Liu et al. 2009), the removal of Zn(II) ions from industrial electroplating wastewater, with a zinc content of 75.5 mg/dm³, was investigated. Mollusc shells were used as the adsorbent, resulting in a high process efficiency of 87% for Zn(II). On the other hand, in a separate study (Šćiban et al. 2007), wood sawdust was used to remove zinc ions from a wire plant effluent with a zinc concentration of 76.3 mg/dm³. The removal efficiencies for Zn(II) ions ranged from 11.2 to 37.5%, depending on the adsorbent dose used.

Based on the results obtained, the sorption capacity for Zn(II) ions by unit mass of the geopolymer was calculated. The coal combustion ash-based geopolymer (PW/GEO)

Table 3. Structure parameters of porous structure of geopolymers after adsorption of Zn(II) ions designated on the basis of low-temperature adsorption and desorption of nitrogen.

	Zn/PW/GEO	Zn/PB/GEO
Surface area [m²/g]		
Single point surface area at P/Po = 0.249	84.98	65.91
BET Surface Area	87.06	68.20
Langmuir Surface Area	121.58	95.79
t-Plot External Surface Area	75.97	65.72
Pore volume [cm³/g]		
Single point desorption total pore volume of pores less than 805.413 Å diameter at P/Po = 0.975	0.198	0.228
BJH Adsorption cumulative volume of pores between 17.000 Å and 3000.000 Å diameter	0.196	0.229
BJH Desorption cumulative volume of pores between 17.000 Å and 3000.000 Å diameter	0.204	0.229
Pore size [Å]		
Desorption average pore width (4V/A by BET)	91.05	133.83
BJH Adsorption average pore diameter (4V/A)	89.53	124.69
BJH Desorption average pore diameter (4V/A)	79.17	105.29

Table 4. Zinc content of post-galvanic sewage sludge before and after the sorption experiment using a geopolymer based on coal combustion ash (PW/GEO) or biomass ash (PB/GEO).

	Content of Zn [g·kg ⁻¹]	Adsorption coefficient [%]	Sorption capacity [mg·g ⁻¹]
before sorption	252.7	-	-
after sorption by PW/GEO	0.004	99.9	4.75
after sorption by PB/GEO	150.0	40.7	1.93

exhibited a higher sorption capacity, with a value of 4.75 mg/g, while the biomass combustion ash-based geopolymer (PB/GEO) showed a sorption capacity of 1.93 mg/g. In comparison, a widely used heavy metal sorbent, activated carbon, typically has sorption capacity values for Zn ranging from 0.004 to 1.04 mg/g (Ugwu and Agunwamba 2020). These results suggest that both geopolymers can be used for the removal of zinc from post-vanning wastes, as they are effective and less expensive compared to activated carbon.

Conclusion

SEM observations revealed significant structural differences in geopolymers after Zn(II) ions adsorption. Porosimetry results confirmed these differences, indicating that mesoporosity prevails in Zn/PB/GEO samples, while microporosity is the predominant type of porosity in Zn/PW/GEO samples. FTIR analysis further supports these findings. In the PB/GEO geopolymer spectrum after the Zn(II) ion adsorption experiment, the disappearance of the band at approximately 1640 cm⁻¹, associated with C=O bond stretching vibrations, implies a reduction in sorption properties. For PW/GEO, changes in intensity and band shifts related to O-H, C-O and N-H stretching vibrations suggest their direct involvement in Zn(II) ion adsorption. The adsorption coefficient for PW/GEO (99.9%) indicates complete Zn(II) ion removal of from galvanic sludge. The high sorption capacity of the studied geopolymers results from electrostatic bonds formed by the reaction between the sorbents' negatively charged surface and zinc cations. FTIR spectroscopic analysis shows the involvement of surface -OH and Si-OH groups during Zn(II) ion binding. Combined with activated carbon, these geopolymers prove to be effective and cost-efficient for removing zinc from galvanic waste, presenting a promising solution.

Based on the obtained results, subsequent studies can be conducted to develop optimal conditions for the removal of zinc from other types of waste. This aims to achieve a relatively clean monometallic waste that can be reused.

References

Adewuyi, Y.G. (2021). Recent Advances in Fly-Ash-Based Geopolymers: Potential on the Utilization for Sustainable Environmental Remediation, *ACS Omega*, 24, pp. 15532-15542. DOI:10.1021/acsomega.1c00662

- Akono, A.T., Koric, S. & Kriven, W.M. (2019). Influence of pore structure on the strength behavior of particle- and fiber reinforced metakaolin-based geopolymer composites, *Cement and Concrete Composites*, 104, pp. 103361. DOI:10.1016/j.cemconcomp.2019.103361
- Alehyen, S., Zerzouri, M., el Alouani, M., el Achouri, M. & Taibi M. (2017). Porosity and fire resistance of fly ash based geopolymer. *Journal of Materials and Environmental Sciences*, 8, pp. 3676-3689
- Ayilara, M.S., Olanrewaju, O.S., Babalola, O.O. & Odeyemi, O. (2020). Waste management through composition: Challenges and Potentials, *Sustainability*, 12, pp. 4456-4479. DOI:10.3390/su12114456
- Barakat, M.A. (2003). The pyrometallurgical processing of galvanizing zinc ash and flue dust, *Journal of Minerals, Metals & Materials Society*, 55, pp. 26-29. DOI:10.1007/s11837-003-0100-4
- Bednarik, M., Vondruska, M. & Koutny, M. (2005). Stabilization/solidification of galvanic sludges by asphalt emulsions, *Journal of Hazardous Materials*, 122, pp. 139-145. DOI:10.1016/j.jhazmat.2005.03.021
- Brylewska, K., Rożek, P., Król, M. & Mozgawa, W. (2018). The influence of dealumination/desilication on structural properties of metakaolin-based geopolymers, *Ceramics International*, 44, pp. 12853-12861. DOI:10.1016/J.CERAMINT.2018.04.095
- Butenegro, J.A., Bahrami, M., Abenojar, J. & Martínez, M.A. (2021). Recent Progress in Carbon Fiber Reinforced Polymers Recycling: A Review of Recycling Methods and Reuse of Carbon Fibers, *Materials*, 14, pp. 6401. DOI:10.3390/ma14216401
- Donohue, M.D. & Aranovich, G.L. (1998). Adsorption hysteresis in porous solids, *Journal of Colloid and Interface Science*, 205, pp. 121-130. DOI:10.1006/jcis.1998.5639
- Dvořák, P. & Jandova, J. (2005). Hydrometallurgical recovery of zinc from hot dip galvanizing ash, *Hydrometallurgy*, 77, pp. 29-33. DOI:10.1016/j.hydromet.2004.10.007
- Galas, D., Kalembkiewicz, J. & Sitarz-Palczak, E. (2016). Physicochemistry, morphology and leachability of selected metals from post-galvanized sewage sludge from screw factory in Łañcut, SE Poland, *Contemporary Trends in Geoscience*, 5, pp. 83-91. DOI:10.1515/ctg-2016-0006
- Jha, M.K., Kumar, V. & Singh R.J. (2001). Review of hydrometallurgical recovery of zinc from industrial wastes, *Resources, Conservation and Recycling*, 33, pp. 1-22. DOI:10.1016/S0921-3449(00)00095-1
- Imtiaz, L., Rehman, S.K.U., Memon, S.A., Khan, M.K. & Javed, M.F. (2020). A review of recent developments and advances in eco-friendly geopolymer concrete, *Applied Sciences*, 10, pp. 7838-7894. DOI:10.3390/app10217838
- Irisawa, T., Iwamura, R., Kozawa, Y., Kobayashi, S. & Tanabe, Y. (2021). Recycling methods for thermoplastic-matrix composites having high thermal stability in focusing on reuse of the carbon fibers, *Carbon*, 175, pp. 605. DOI:10.1016/j.carbon.2021.01.042
- Jeyasundar, P.G.S.A., Ali, A. & Zhang, Z. (2020). Waste treatment approaches for environmental sustainability, *Microorganisms for Sustainable Environmental and Health*, 6, pp. 119-135. DOI:10.1016/B978-0-12-819001-2.00006-1
- Khan, M.N.N., Kuri, J.C. & Sarker, P.K. (2021). Effect of waste glass powder as a partial precursor in ambient cured alkali activated fly ash and fly ash-GGBFS mortars, *Journal of Building Engineering*, 34, pp. 101934-101945. DOI:10.1016/j.conbuildmat.2020.120177

- Kriven W.M., Bell J.L. & Gordon M. (2006). Microstructure and Microchemistry of Fully-Reacted Geopolymers and Geopolymer Matrix Composites. In: Bansal, N.P., Singh, J.P., Kriven, W.M., Schneider, H., *Advances in Ceramic Matrix Composites IX* (pp. 227-250). The American Ceramic Society, Wiley, New York 2006.
- Krishnan, S., Zulkapli, N.S., Kamyab, H., Taib, S.M., Bin Md Din, M.F., Majid, Z.A., Chairapat, S., Kenzo, I., Ichikawa, Y., Nasrullah, M., Chelliapan, S. & Othman, N. (2021). Current technologies for recovery of metals from industrial wastes: An overview, *Environmental Technology & Innovation*, 22, pp.101525. DOI:10.1016/j.eti.2021.101525
- Król, M., Rożek, P., Chlebda, D. & Mozgawa, W. (2018). Influence of alkali metal cations/type of activator on the structure of alkali-activated fly ash - ATR-FTIR studies, *Spectrochim. Acta Part A: Molecular and Biomolecular Spectroscopy*, 198, pp. 33-37. DOI:10.1016/j.saa.2018.02.067
- Krstić, I., Zec, S., Lazarević, V., Stanisavljević, M. & Golubović, T (2018). Use of sintering to immobilize toxic metals present in galvanic sludge into a stable glass-ceramic structure, *Science of Sintering*, 50, pp. 139-147. DOI:10.2298/SOS1802139K
- Kwon, O-S. & Sohn, I.L. (2020). Fundamental thermokinetic study of a sustainable lithium-ion battery pyrometallurgical recycling process, *Resources, Conservation and Recycling*, 158, pp. 104809. DOI:10.1016/j.resconrec.2020.104809.
- Letcher, R.M. & Vallerio, D.A. (2019). *Waste. A Handbook for Management*, 2, pp. 585-630. DOI:10.1016/B978-0-12-381475-3.10034-8
- Li, M., Xu, J. & Li, B. (2018). Analysis of development of hazardous waste disposal technology in China, *IOP Conf. Series: Earth and Environmental Science*, 178, pp. 1-7. DOI:10.1088/1755-1315/178/1/012027
- Luo, X., Liu, G., Xia, Y., Chen, L., Jiang, Z., Zheng, H. & Wang, Z. (2017). Use of biochar-compost to improve properties and productivity of the degraded coastal soil in the Yellow River Delta China, *Journal of Soil and Sediments*, 17, pp. 780-789. DOI:10.1007/s11368-016-1361-1
- Luukkonen, T., Runtti, H., Niskanen, M., Tolonen, E., Sarkkinen, M., Kemppainen, K., Rämö, J. & Lassi, U. (2016). Simultaneous removal of Ni(II), As(III), and Sb(III) from spiked mine effluent with metakaolin and blast-furnace-slag geopolymers, *Journal of Environmental Management*, 166, pp. 579-588. DOI:10.1016/j.jenvman.2015.11.007
- Luz, C.A., Rocha, J.C., Cheriaf, M. & Pera, J. (2009). Valorization of galvanic sludge in sulfoaluminate cement, *Construction and Building Materials*, 23, pp. 595-601. DOI:10.1016/j.conbuildmat.2008.04.004
- Makisha, N. & Yunchina, M. (2017). Methods and solutions for galvanic waste water treatment, *MATEC Web of Conferences*, 106, pp. 1-6. DOI:10.1051/mateconf/201710607016
- Nanda, S. & Berruti, F. (2021). Municipal solid waste management and landfilling technologies: a review, *Environmental Chemical Letter*, 19, pp. 1433-1456. DOI:10.1007/s10311-020-01100-y
- Pu, S., Duan, P., Yan, C. & Ren, D. (2016). Influence of sepiolite addition on mechanical strength and microstructure of fly ash-metakaolin geopolymer paste. *Advanced Powder Technology*, 27, pp. 2470-2477. DOI:10.1016/j.appt.2016.09.002
- Riaz, M., Bing Chen, A., Aminul Haque, M. & Shah, S.F.A. (2020). Utilization of industrial and hazardous waste materials to formulate energy-efficient hygrothermal biocomposites, *Journal of Cleaner Production*, 250, pp. 119469. DOI:10.1016/j.jclepro.2019.119469
- Rossini, G. & Bernardes, A.M. (2006). Galvanic sludge metals recovery by pyrometallurgical and hydrometallurgical treatment, *Journal of Hazardous Materials*, 131, pp. 210-216. DOI:10.1016/j.jhazmat.2005.09.035.
- Rudnik, E. (2019). Investigation of industrial waste materials for hydrometallurgical recovery of zinc, *Minerals Engineering*, 139, pp. 105871. DOI:10.1016/j.mineng.2019.105871
- Rybak, J., Gorbatyuk, S.M., Bujanovna-Syuryun, K.C., Khairutdinov, A., Tyulyaeva, Y. & Makarov, P.S. (2021). Utilization of Mineral Waste: A Method for Expanding the Mineral Resource Base of a Mining and Smelting Company, *Metallurgist*, 64, pp. 851-861. DOI:10.1007/s11015-021-01065-5
- Sanito, R.C., Bernuy-Zumaeta, M., You, S-J. & Wang Y-F. (2022). A review on vitrification technologies of hazardous waste, *Journal of Environmental Management*, 316, pp. 115243. DOI:10.1016/j.jenvman.2022.115243
- Sinha, S., R. Choudhari, R., Mishra, D., Shekhar, S., Agrawal, A. & Sahu, K.K. (2020). Valorisation of waste galvanizing dross: Emphasis on recovery of zinc with zero effluent strategy, *Journal of Environmental Management*, 256, pp. 109985. DOI:10.1016/j.jenvman.2019.109985
- Sitarz-Palczak, E.; Kalembkiewicz, J. & Galas, D. (2019). Comparative study on the characteristics of coal fly ash and biomass ash geopolymers, *Archives of Environmental Protection* 45, pp. 126-135. DOI:10.24425/aep.2019.126427
- Stepanov, S., Morozov, N., Morozova, N., Ayupov, D., Makarov, D. & Baishev, D. (2016). Efficiency of Use of Galvanic Sludge in Cement Systems, *Procedia Engineering*, 165, pp.1112-1117. DOI:10.1016/j.proeng.2016.11.827
- Świerk, K., Bielicka, A., Bojanowska, I. & Maćkiewicz, Z. (2007). Investigation of Heavy Metals Leaching from industrial wastewater sludge, *Polish Journal of Environmental Studies*, 16, pp. 447-451.
- Šćiban, M., Radetić, B., Kevrešan, Z. & Klačnja, M. (2007). Adsorption of heavy metals from electroplating wastewater by wood sawdust, *Bioresource Technology*, 98, pp. 402-409. DOI:10.1016/j.biortech.2005.12.014
- Toledo, M., Siles, J.A., Gutierrez, M.C. & Martin, M.A. (2018). Monitoring of the composting process of different agroindustrial waste: influence of the operational variables on the odorous impact, *Waste Management*, 76, pp. 266-274. DOI:10.1016/j.wasman.2018.03.042
- Ugwu, E.I. & Agunwamba, J.C. (2020). A review on the applicability of activated carbon derived from plant biomass in adsorption of chromium, copper, and zinc from industrial wastewater, *Environmental Monitoring and Assessment*, 192, pp. 240-252. DOI:10.1007/s10661-020-8162-0
- Yang, J., Firsbach, F. & Sohn, I.L. (2022). Pyrometallurgical processing of ferrous slag “co-product” zero waste full utilization: A critical review, *Resources, Conservation and Recycling*, 178, pp. 106021. DOI:10.1016/j.resconrec.2021.106021
- Zehua, J., Liya, S. & Yuansheng, P. (2020). Synthesis and toxic metals (Cd, Pb, and Zn) immobilization properties of drinking water treatment residuals and metakaolin-based geopolymers, *Materials Chemistry and Physics*, 242, pp. 1-9. DOI:10.1016/j.matchemphys.2019.122535

Badania usuwania jonów cynku z osadów galwanicznych przez geopolimery

Streszczenie. Osady galwaniczne zawierają szereg toksycznych metali ciężkich, które w warunkach środowiskowych mogą być mobilne jako chemicznie aktywne jony. W pracy badano możliwość wykorzystania geopolimerów na bazie popiołów lotnych do usuwania jonów Zn z osadu galwanizacyjnego. W pracy do usuwania Zn z galwanicznych osadów ściekowych wykorzystano geopolimery przygotowane metodą geopolimeryzacji. Zastosowano dwa rodzaje geopolimerów, otrzymywane na bazie popiołów ze spalania węgla i popiołów ze spalania biomasy. Strukturę, morfologię i właściwości powierzchni scharakteryzowano odpowiednio za pomocą FTIR i SEM. Dodatkowo wyznaczono izotermę BET i Langmuira oraz przeprowadzono analizę tych izoterm dla ciał porowatych (metoda t-Plot i metoda BJH). Wykazano, że geopolimer otrzymany z popiołów ze spalania węgla jest skuteczniejszym sorbentem dla jonów Zn(II). Skuteczność usuwania jonów Zn(II) dla geopolimeru na bazie popiołów ze spalania węgla wynosi 99,9%, a dla geopolimeru na bazie popiołów ze spalania biomasy 40,7%. Otrzymane rezultaty są wynikiem powstawania wiązań pomiędzy grupami -OH i/lub Si-OH obecnymi na powierzchni zastosowanych geopolimerów a jonami Zn(II), których obecność stwierdzono na podstawie analizy widm FTIR. Procedura ta jest korzystna z ekologicznego i ekonomicznego punktu widzenia ponieważ zapewnia maksymalny odzysk cennego składnika przy możliwie najniższych kosztach. Ponadto, pozwala na uzyskanie stosunkowo czystych odpadów monometalicznych, które można ponownie wykorzystać.